Heritage Science

RESEARCH

Open Access

Condition and characterization analysis of a twentieth century cultural heritage through non-destructive testing (NDT) methods: the case of the Sivas industry school ironworking atelier in Turkey

Gamze Fahriye Pehlivan*

Abstract

Before the conservation and restoration of many types of cultural heritage, it is necessary to perform careful examination. This study aimed to determine the original building state and deterioration by applying non-destructive testing (NDT) methods in the case of a heritage building. Another goal was to determine, via NDT methods, whether the limestones observed in this study of different forms, colours, and textures were truly different. The Sivas Industry School Ironworking Atelier, which constitutes the research object, is one of the important public buildings in the city of Sivas, Turkey. Within the scope of the study, non-destructive infrared thermography (IRT), Schmidt hammer rebound (SHR) tests, and X-ray fluorescence (XRF) spectroscopy were applied. Accordingly, through IRT, deteriorations, anomalies, and material differences were investigated, and via SHR testing, uniaxial compressive strength (UCS) estimates, strength levels and hardness classes of stones were obtained. Moreover, via XRF spectroscopy, characterization analysis of stones was conducted. The data obtained could provide information to establish a basis for subsequent conservation. The innovation of this study is that although the infrared thermography technique is typically used in the investigation of materials, it was revealed that another technique such as XRF analysis is needed to better determine whether stones that seem different based on IRT are actually different. With IRT technique, anomaly and material detorioration can be determined. In addition to these two techniques, SHR tests that are non-destructive methods are needed to think about mechanical features of the material. Therefore, when determining the conditions and for characterization analysis of a cultural heritage before restoration, different techniques should be jointly used to complement each other.

Keywords Sivas Archeology Museum, XRF, Infrared thermography, Schmidt hammer tests, Sivas ındustry school ıronworking atelier, NDT

Introduction

Sustainable preservation of cultural heritage can be ensured through periodic maintenance and repair activities. With maintenance and simple repairs, such as periodically checking rain gutters, immediately removing leaves, shrubs, soil, bird droppings, etc., accumulated in gutters, immediately reinstalling dislodged tiles, renovating corroded chains, repairing roof damage, repainting in

*Correspondence:
Gamze Fahriye Pehlivan
geraybat@hotmail.com
Department of Architecture, Sivas Cumhuriyet University, Sivas, Turkey

the case of paint and whitewash problems, plaster crack filling, cleaning the façade using the appropriate method in the presence of pollution, building problems can be solved in a timely manner, without the need for major repairs. Thus, less building intervention will be required, and lower costs will be incurred.

However, in cases where periodic maintenance is not conducted due to the inability to allocate funds or budget inadequacy, apathy, lack of adequate technical personnel in organizations responsible for maintenance, and difficulty due to legal procedures, deterioration of buildings can ensue. In some cases, deterioration occurs due to reasons arising from the first construction phase of the building, or nearby new constructions, well drilling/closure, road construction, tunnel construction, heavy vehicle traffic, air pollution, user interventions, obsolete or improper installations, vandalism, terrorism, natural disasters, fires, and exposure to long-term atmospheric conditions, regardless of periodic maintenance [1].

The determination of cultural heritage deterioration is important to implement appropriate safeguards, to stop the deterioration process, or to eliminate deterioration. Correct solution suggestions should be obtained via accurate examination and diagnosis. There are numerous test methods for deterioration detection, destructive or non-destructive. Considering that the building in question is a cultural heritage, the historical value, evidential value, artistic (aesthetic) value, authenticity, and integrity of the building must be preserved.

Today, restoration specialists also recommend non-destructive testing (NDT) methods. Some of the NDT techniques are X-ray fluorescence spectroscopy, raman spectroscopy, terahertz (THz) technology, infrared thermography, flash thermography sound absorption, sonic/ultrasonic, electromagnetic and electrical techniques, Schmidt Hammer Rebound (SHR) test. Owing to the development of NDT methods, there is no need to collect samples at sites [2–11]. Considering the reasons described above, it could be determined that this decision was correct. Therefore, this study aimed to promote and guide the determination of cultural heritage deterioration and identify problems by using non-destructive testing methods.

Within the scope of this study, visible problems such as cracks, pores, blistering of plaster, plant growth, and invisible anomalies underneath plaster were examined. In addition, this study aimed to detect different building materials and plaster-covered anomalies with a thermal camera and to obtain determinations regarding the original state of the building.

To provide accurate solutions to these problems, the building materials of cultural heritage elements must also be correctly determined. Another purpose of this article was to encourage elemental analysis of the structure of materials. Within this context, characterization analysis was performed without building sampling or destruction to better determine whether building stones that appear different actually differed.

What is more, Schmidt hammer rebound tests were applied to get an idea about the mechanical features of the material without taking any samples. As a result of these tests, approxiemate UCS values are estimated. From the estimated UCS values, the strength and hardness classes of the stones were determined.

The studies executed within the scope of this article constitute preliminary studies that form a basis for cultural heritage restoration. In other words, restoration should not be conducted without these investigations.

Materials and methods

Materials

The research object of this study is the Sivas Industry School Ironworking Atelier located at the Sivas provincial centre in Turkey (Figs. 1, 2, 3). This is a cultural heritage building registered by the Regional Council for the Conservation of Cultural Property on 22.07.1983 with registration decision A-4468 [12]. This building was chosen as an example because it is one of the outstanding Sivas examples of keeping up with the Industrial Revolution. This public building indicating a cross-section of twentieth century architecture should be conserved and meticulously passed down to future generations. As the first step of the conservation, the building should be well-defined. Accurate identification and deterioration of the building materials is a preliminary preparation for the next stage, restoration. Since the geography, climate and geology are known to shape the architecture and affect deterioration, it is necessary to address these issues via an overview before examining this cultural heritage building.

Geography, climatic conditions, and general geology of the study area

Sivas has an altitude of 1285 m and is located in the basin of the Kizilirmak River, which is a very important river for this city [13, 14]. The city, which is located in a region with a descending topography, starts from the foot of the Meraküm Plateau. The Mismil River, Murdar River, and Pünzürük Creek (Kale River) pass through this city. The Murdar River, which flows along the north–south axis, connects to the Mismil River in the southeast. The Mismil River in the east of the city also merges with the Kizilmak River [15]. The Pünzürük Creek also flows from the northwest to the southwest of the city and merges with the Kizilmak River.

Fig. 1 Location of Sivas in Turkey [18]

The mountain ranges to the north and south of Sivas significantly impact the climate in the region. To the south occur Tecer Mountain, Gürleyik Mountain, Bey Mountain, Bozbel Mountains, Kılıç Mountain, Büyük Yılanlı Mountain, and Çengelli Mountain, and to the north occur Köse Mountains, Kızıl Mountain, BüyükKızıl Mountain, Tekeli Mountain, Asma Mountain, and Toraç Mountain (Fig. 2). The Uzunyayla Plateau in the southwest and the Meraküm Plateau at the centre are important morphological formations in Sivas. The plain areas are relatively small and surrounded by mountains [16, 17].

In Sivas, which is geographically shaped by streams, high plateaus, and mountains, a harsh terrestrial climate can be observed. In Sivas, the lowest temperature measured over the last 90 years is − 34.4 °C, the highest temperature is + 40 °C, the average sunshine duration is 6.8 h, the wind speed is no more than 41.2 m/s, the highest snow level is 110 cm, and the highest daily precipitation is 55.0 mm. In addition, the temperature difference between day and night is large [19].

In and around Sivas, the gypsum layer is widespread, along with limestone layers [20]. In addition, Sivas, which contains the only operating strontium mine in Turkey, provides iron, chrome, lead–zinc, cement raw materials, and talc fields [21]. In addition, there occur travertine and marble deposits and granite–cyanite, breccia, andesite–basalt, and limestone occurrences that can be used as building materials [22]. The large number of quarries has been instrumental in the use of ashlar in historical public buildings in Sivas and in certain historical buildings built by the wealthy.

Architecture of the Sivas ındustry school ıronworking atelier

At the historical city centre of Sivas, there are important public buildings such as madrasahs, inns, mosques, gendarmerie buildings, libraries, and governor offices. Another surviving public building is the Industry School and its atelier (Fig. 3).

The Industry School, first proposed by Governor Hadji Hasan but not completed, was founded by Rashid Akif Pasha. The school was later developed by Governor Muammer Bey by adding ironworks, carpentry, and carpet ateliers [23–25]. The building that constitutes the subject of this study is the ironworks atelier, which is located just southwest of the Industry School and was used in contingent with the school. The main entrance of the building, located in the corner parcel, occurs in Rahmi Günay Street in the east. Entrances are also located on the western, northern, and southern fronts. There are roads around all three sides of the parcel where the building is located (Fig. 3).

The building, which is one of the important representatives of the Sivas National Architectural Movement, was built in 1914 according to an inscription and served for many years as an application atelier belonging to the

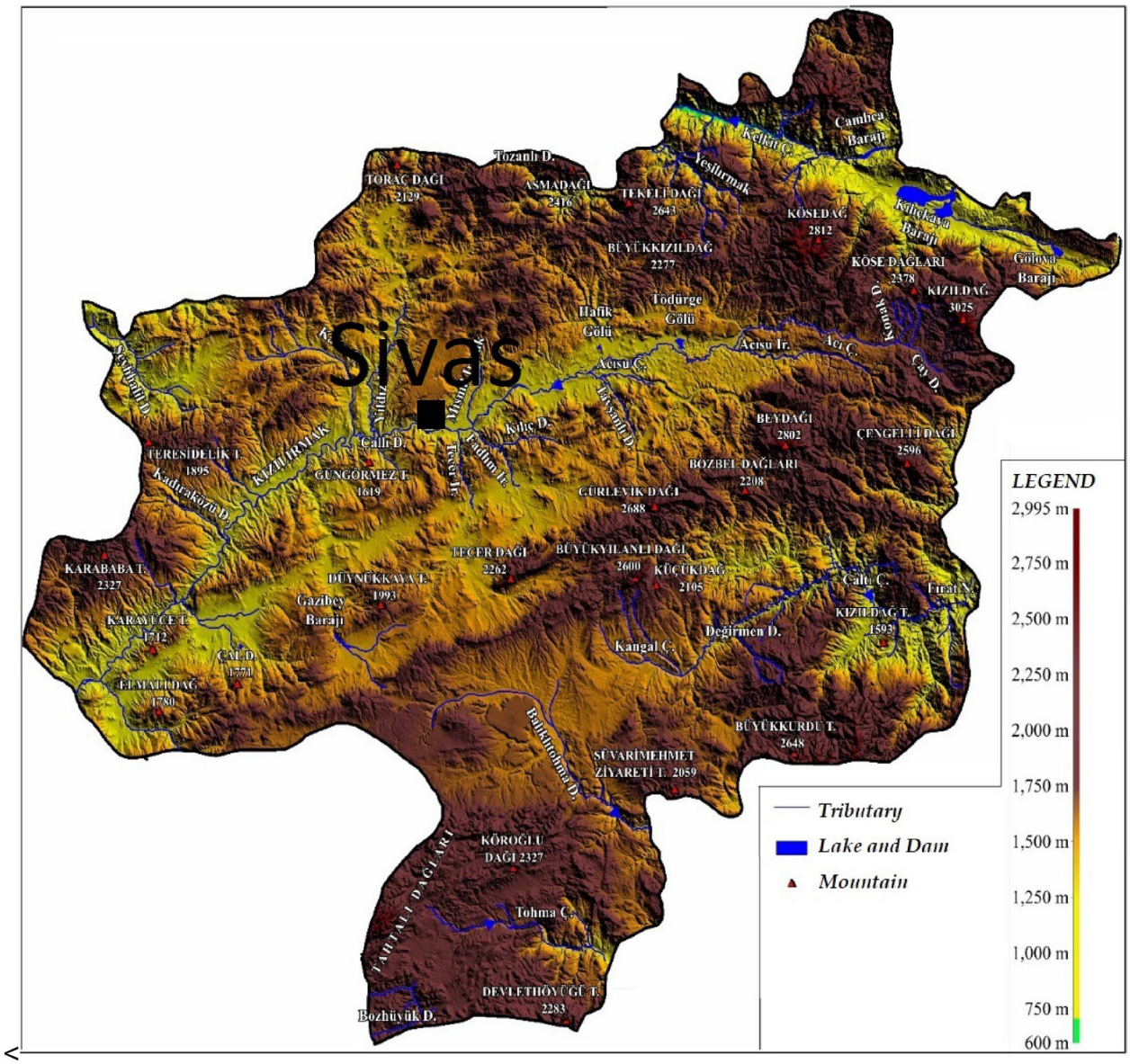

Fig. 2 DEM (Digital Elevation Model) map of Sivas [17]

Industry School. In later years, it served as a school affiliated with the Ministry of National Education, along with other surrounding annexes. In 1996, these additional buildings around the school were demolished. The building also experienced a fire in the past. Until 2003, the building was used as the woodworking atelier of the Sivas Industrial Vocational High School under the Ministry of National Education. It was restored from 2005 to 2007. Since 2009, it has continued to be used as an archaeological museum [12, 23–26].

On the eastern façade of the northern wing of the building, at the foundation level, there are 3 rows of pitch-faced stones, 2 rows of ashlar above them, and plaster and yellow paint on the rows of ashlar. At the foundation level on the southern flank of this façade, there are no pitch-faced stones and only 5 rows of ashlar. Due to the elevation difference, the building can be entered via five steps. To the right and left of the entrance door are pseudo-columns and column heads of symmetrically smooth ashlar. The door jamb continues above these elements. There is an inscription on the forehead formed by the jamb (Fig. 4). The gates in the north and south exhibit similar characteristics.

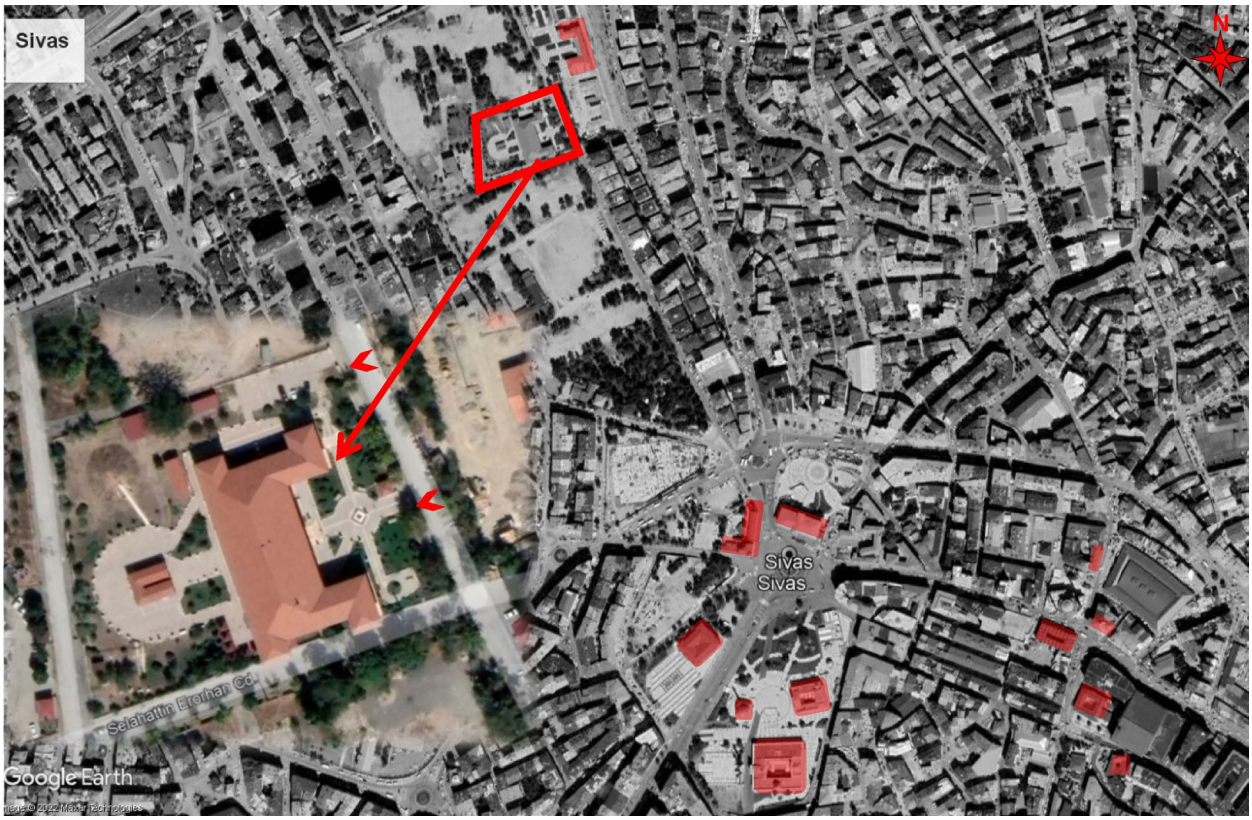

Fig. 3 Sivas historical city centre and location of the Industry School Ironworking Atelier [18]

Fig. 4 Eastern facade of the Industry School Ironworks Atelier (panoramic photo)

In the corners to the north and south of the U-plan building, the spaces projected from the plan stand out. The façades of these spaces were built with ashlar up to the moulding level. The mouldings, corners, window casings, and window sills of the building are also constructed of ashlar. The windows are tangential arches, and the doors on the eastern, southern, and northern fronts are depressed arches. The wide eaves of the hipped roof building are supported by angle braces (Fig. 4) [23, 27].

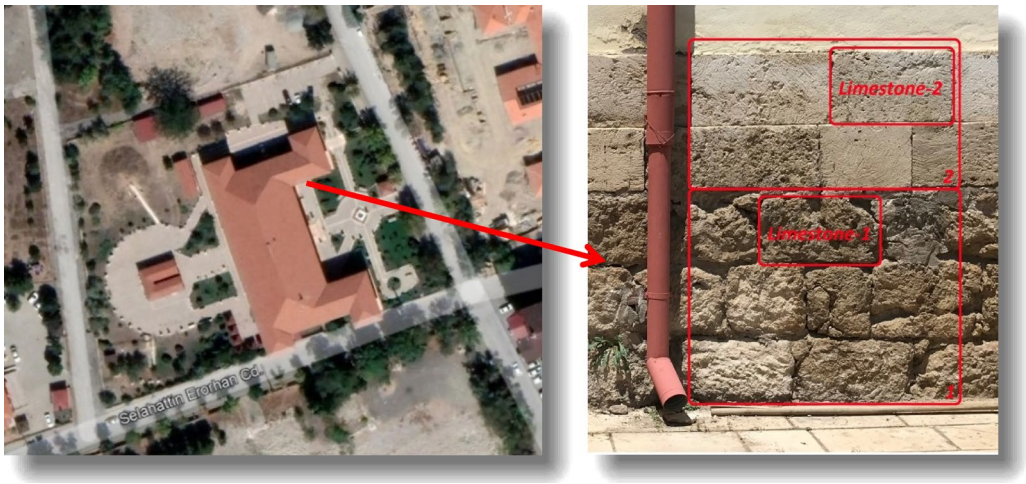

Fig. 5 Wall where the Schmidt hammer rebound (SHR) test was performed [18]

Methods

Within the scope of this study, the infrared thermography (IRT) method, an NDT method [28], was used to detect deteriorations, anomalies, and material differences. In addition, Schmidt hammer rebound (SHR) tests were performed to obtain UCS estimates and strength and hardness classes of the stones, and X-ray fluorescence (XRF) spectroscopy was used for characterization analysis.

Infrared thermography

Thermography dates back to the discovery of infrared radiation by William Herschel in 1800 [29–31]. Later, this technique was developed by scientists and was used in different fields related to architecture and engineering, such as detection of problems of buildings such as cracks, detachments, flaking, voids in detail combinations, humidity, determination of spatial comfort levels in open and closed areas, material research, determination of building materials underneath plaster, preparation of fire risk analysis, calculation of thermal gains from insolation, and calculation of the thermal insulation efficiency, thermal performance, heat transfer, heat flux rate and thermal conductivity [32–52].

One of the uses of the IRT technique is non-destructive testing of cultural heritage elements [28, 32, 53, 54]. A thermal camera detects infrared radiation emitted by objects and converts them into temperature data and visualizes these data in the form of colour thermal maps on a certain scale [31]. With this method, it is possible to detect damage, defects, or material differences that are invisible or difficult to observe with the naked eye.

In this study, an infrared thermal camera was used within the resolution range from 7.5 to 14 µm. The camera with a sensitivity of 0.1 °C and a temperature range from − 20 °C to + 1000 °C is a Trotec IC080 LV camera. During image recording, images of 627 × 410 pixels were obtained. Digital camera images were also obtained at locations where thermal images were recorded. With a digital camera, 4032 × 3024 pixel photos were obtained.

According to a literature review, to obtain efficient results from thermal camera measurements, it is recommended that shooting should be conducted either on a cloudy day without rain or at sunrise/sunset in summer or at night in winter [44, 47, 55–59]. One of the most important reasons for this approach is the interference due to sunshine [55].

Shooting occurred on a cloudy day on June 12, 2021. The wind speed was 1.67 m/s, the temperature ranged from 10 to 24 °C, and the humidity was 36% [60, 61]. It is not desirable to have a high wind speed during thermal camera operation. Excessive wind may cause moisture evaporation on the surface and make it difficult to detect problems due to moisture. The wind speed should be less than 5–10 m/s [47, 56, 57]. On the day of thermal camera measurement, the wind speed was suitable.

In regard to the deterioration types determined by the thermal camera and to ensure compliance with the general terminology and facilitate the establishment of a suitable scientific framework, the terms in the dictionary prepared by the ICOMOS International Scientific Committee for Stone (ISCS) on stone deterioration were used [62]. This article includes an example of the different types of deterioration issues detected during thermal imaging.

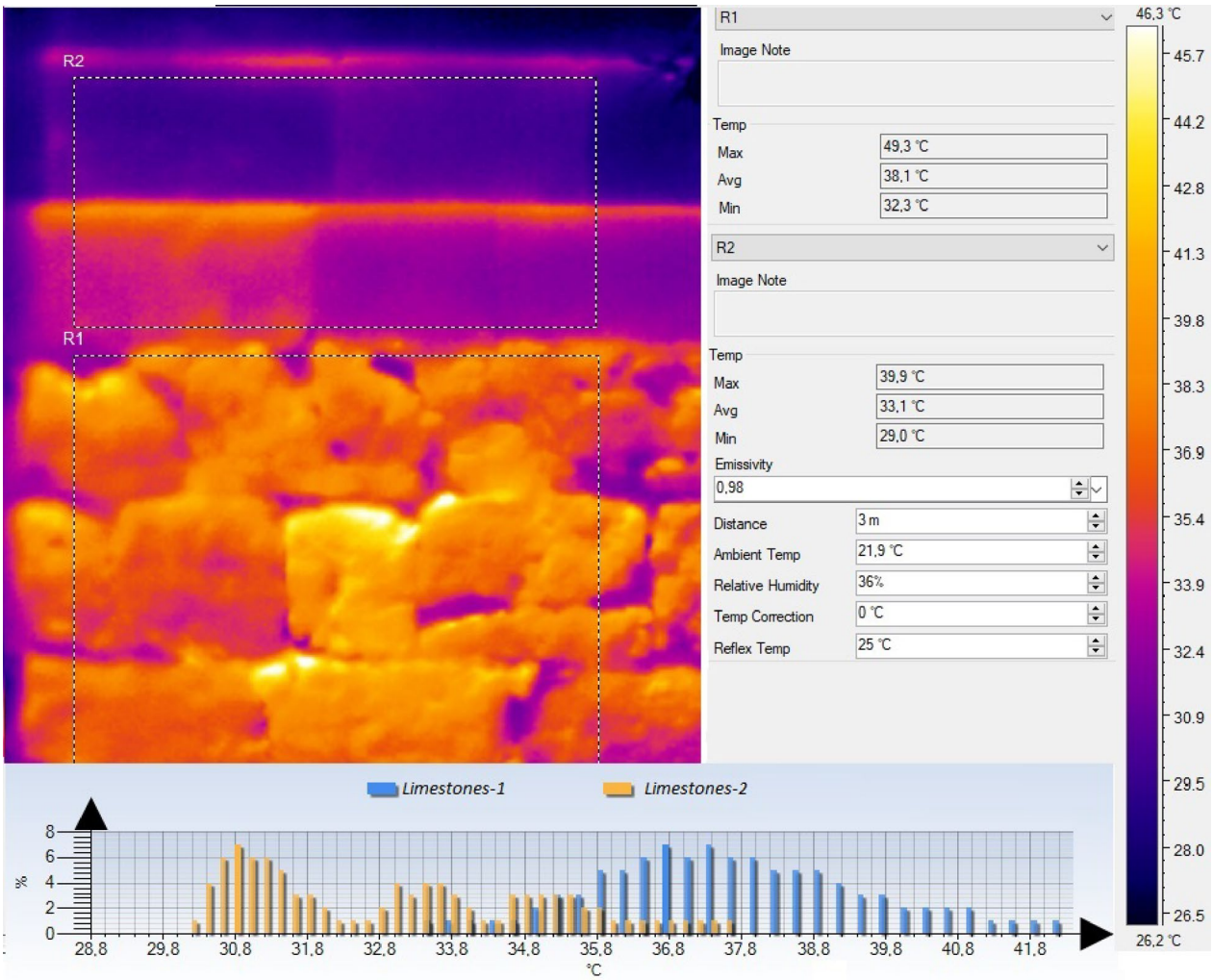

Fig. 6 Graphic of the surface temperature of limestone-1 and limestone-2

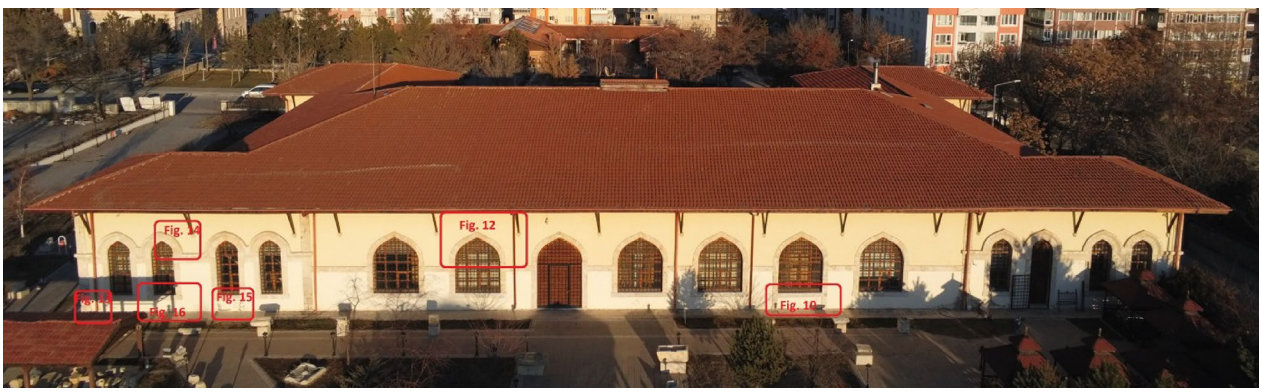

Fig. 7 Western facade of the Industry School Ironworks Atelier

Schmidt hammer rebound (SHR) tests

The uniaxial compressive strength (UCS) is one of the important indicators used to determine the strength and life of stones. Obtaining core samples from a heritage building and conducting UCS experiments can unfortunately damage cultural heritage, although the

Fig. 8 Northern facade of the Industry School Ironworks Atelier

Fig. 9 Southern facade of the Industry School Ironworks Atelier

right results can be obtained [63–65]. Instead, one of the non-destructive testing methods of cultural heritage, the Schmidt hammer rebound (SHR) test method, can be used [66–69]. This method saves both time and cost. There is no need for a special laboratory.

The Schmidt hammer was originally developed to determine the strength of concrete [70] and was later used to obtain hardness and strength classes of rocks [69, 71–75]. The hammer works simply given the principle of piston recoil of a compressed spring. The amount of recoil is obtained from the device.

There are 2 types of Schmidt hammers commonly used for rocks, N- and L-type hammers. The N-type hammer can be used for both weak and strong rocks while delivering higher impact energy. The L-type hammer is suitable for weaker rocks [63, 75, 76]. In the experiment, an N-type JE IL Precision Industrial Instrument JI-355 Schmidt hammer was used.

The pitch-faced stones in zone 1 were denoted as limestone-1, and the ashlar in zone 2 was denoted as limestone-2 (Fig. 5). As shown in the photo, the stones in these two zones differ. For this reason, Schmidt hammer rebound (SHR) tests were performed involving both zones. With the Schmidt hammer, 10 strokes were made to the marked stones with Schmidt hammer in Fig. 5. The numerical data obtained as a result of the applied strokes were recorded as SHR values.

X-Ray fluorescence (XRF) spectroscopy

X-ray fluorescence (XRF) spectroscopy is an NDT method used to determine the elemental composition. This method has been proven to be reliable and valid and has recently been preferred in analysis studies for the preservation of many cultural heritages [2, 7, 10, 77–81].

In this study, a Thermo Scientific Niton XL3 portable XRF device was used. The use of the portable XRF device eliminated the need to collect samples from the building. No contact was made with the stones, and the device collected data from a distance of 1 mm.

As mentioned above, since the appearance of stones in the 1st and 2nd regions differed, elemental analysis with XRF was performed of both types of stones (Fig. 5). Thus, we aimed to determine whether limestone-1 and limestone-2 differed. The stones whose XFR analysis were

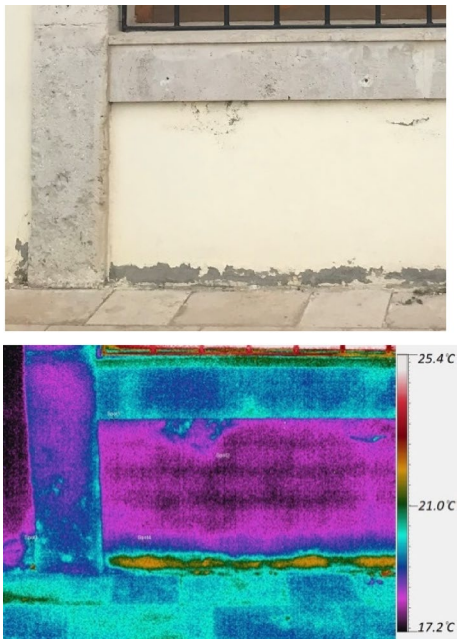

Fig. 10 Different material underneath the plaster layer

Fig. 11 Capillary crack due to material difference

made in the 1st and 2nd regions were marked in Fig. 5 and before starting the study, dust and dirt were removed from the surface.

Results and discussion

Infrared thermography

The infrared thermography method enables the detection of problems such as cracks, crevices, joint gaps, material loss, moisture in walls, different building materials, and anomalies hidden underneath plaster. For this purpose, thermal camera measurements of the stones in the 1st and 2nd zones were obtained to detect possible building material differences. The thermal camera software was used to calculate the average surface temperature in these two zones, and this value averaged 38.1 °C for the stones in the 1st zone and 33.1 °C for the stones in the 2nd zone (Fig. 6). There was a difference of 5 °C between these two zones. Because there are many stones in 1st and 2nd regions, taking the temperature average of the stones will provide a better comparison since this will minimize the effect of undesirable factors that change the temperature (like pore, wind, roughness, shape of the stone, etc.)

As a result of IRT scanning of the building, anomalies could be detected underneath plaster (Figs. 7, 8, 9). Although it is known that the building is constructed of stone, the thermal image in Fig. 10 shows that underneath the plaster layer, different material than stone (possibly brick?) was used in the building. This indicates that this window was once used as a door, filled with various materials during the restoration phase and converted into a window. In addition, there occurred paint spills and plaster blisters on the wall surface.

Another anomaly is shown in Fig. 11. In the digital camera image, a very thin capillary crack could be visible. The cause of this difficult-to-notice problem could be determined with the help of the thermal camera image. The appearance of temperature differentiation on the same wall surface indicated that different materials were used in these two regions. The material difference caused these two surfaces to independently operate, creating a capillary crack in the plaster layer.

Figure 11 shows that the different building materials, seemingly with or without any deterioration, were not visible to the naked eye and occurred below the plaster layer but could be detected via the IRT method. The wooden beam, which continues along the horizontal line under the eave, was not observed in the digital camera image but could be detected with the thermal camera. This image emerged due to the difference between the thermal conductivity coefficient of the wooden beam and that of the stone wall (Fig. 12).

Scanning of the building façades with the thermal camera continued. Thermal images were also obtained at locations with visible defects. In this article, one example of each defect is presented to conserve space. Figure 13 shows limestone splitting along the plane of weakness due to overload. As shown in Fig. 14, pores in limestone could be observed, and plaster blistering and falling are shown in Fig. 15. Small air gaps formed due to cracks, pores, plaster blistering, and material

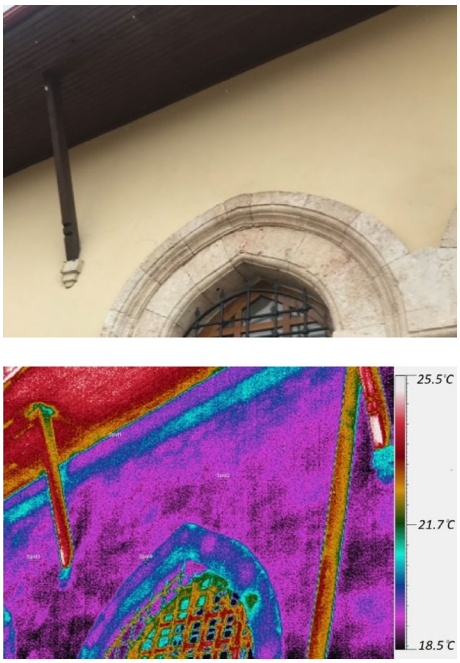

Fig. 12 IRT detection of invisible building materials underneath plaster

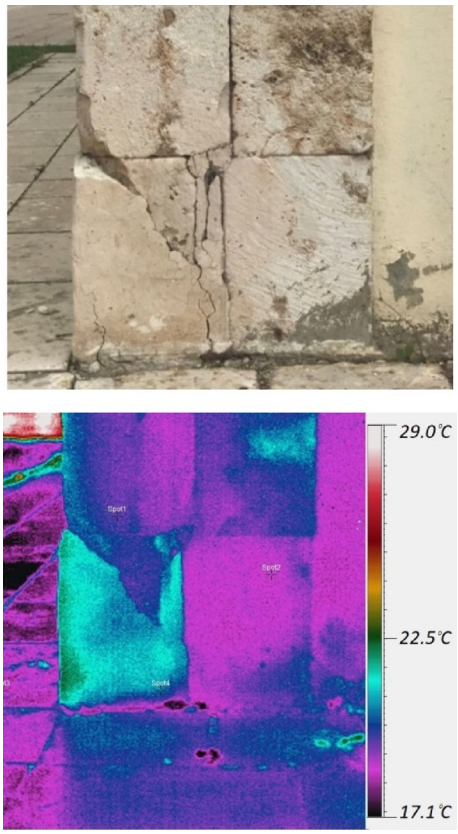

Fig. 13 Splitting of limestone along the plane of weakness because of overload

shedding. There was also a temperature difference between the air gap and the building material. Since these features trapped dry air, small gaps such as pores, cracks, and plaster swells were not affected by the low atmospheric temperature during the morning hours, similar to the principle of operation of thermal insulation materials. Therefore, since the air trapped in these gaps exhibits a lower thermal conductivity than that of the building materials, the temperature in the air gaps was higher.

Figure 16 shows that the limestone of the window sill was blistered at Point a, and this blistered piece fell. Since the part that fell is very large in size, dry air was not trapped, similar to small porous thermal insulation materials. In contrast, this region exhibited a lower temperature than that of the building material, as the humid air accumulated here increased heat transmission via conduction. Figure 15 shows that this area was warmer than the other surfaces, as described above, since there are small pores at Point b.

As an unqualified intervention shown in Fig. 17, part of the wall was plastered with cement plaster, and the surface temperatures differed because of the different thermal conductivity coefficients of cement plaster and stone. In addition, as shown in the digital image, plants grew at the junction of the wall and ground level. These plants, which grow uncontrolled between the joints of the stones or on the surface where the wall meets the ground level, could damage the stone due to their acidic effect. Even if the roots of these plants were weak, they could create problems such as maintaining moist stones and causing salt accumulation [62].

Schmidt hammer rebound (SHR) tests

There are numerous recommendations in the literature regarding the evaluation of Schmidt hammer test results. The vast majority of these are based on the elimination of suspicious values, large or very small, and then averaging the remaining values [82–86].

In this study, R values obtained from the Schmidt hammer test were evaluated according to ASTM 2019 guidelines. On the same stone, 10 readings were recorded, and the average value was calculated. Values 7 units below and above the average were excluded from the assessment [83]. A total of three values were excluded from the evaluation, and the average was recalculated.

De Beer (1967) determined hardness classes of rocks according to Schmidt hammer rebound (SHR) values [71]. According to the average SHR values of limestone-1 and limestone-2, the hardness classification of the stones is given in Table 1.

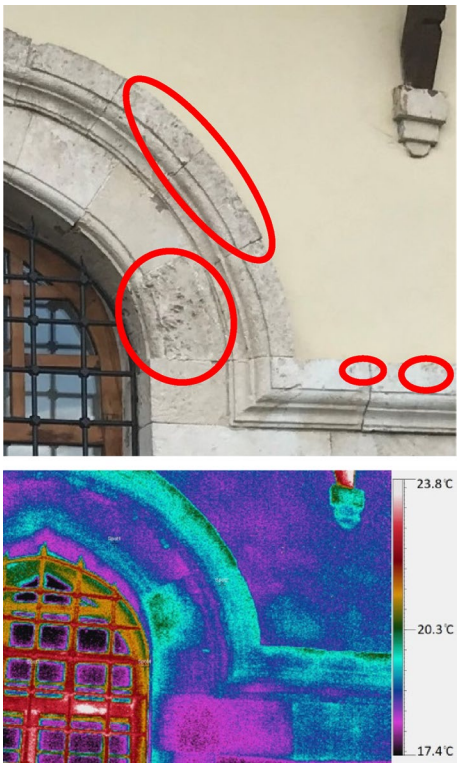

Fig. 14 Pores in limestone

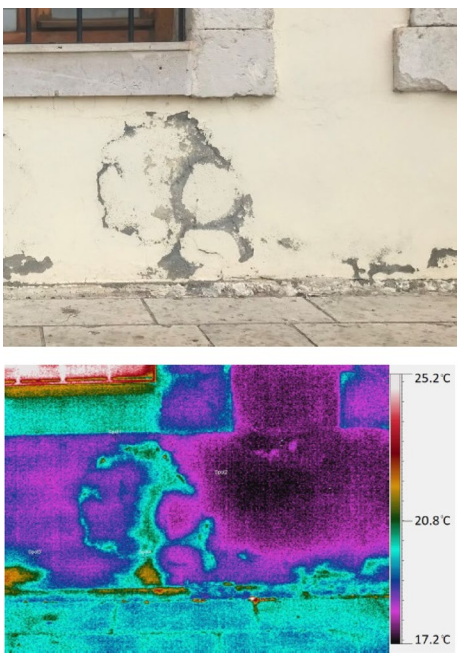

Fig. 15 Blistering of plaster

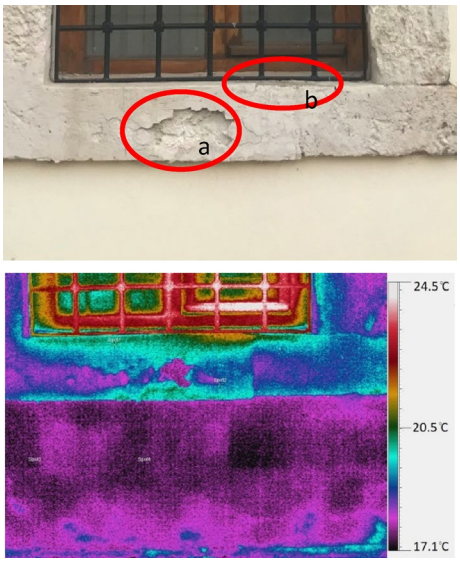

Fig. 16 **a** Blistering of the limestone window sill;**b** pores in limestone

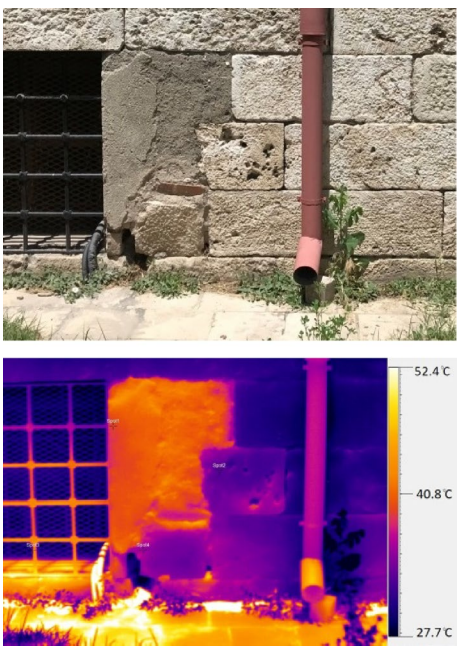

Fig. 17 Detection of plant growth and material differences with the thermal camera

The SHR test method was also used to provide insight into the uniaxial compressive strength (UCS) of the stones. Numerous equations have been developed to minimize errors in the conversion of SHR values into UCS values. Only transformation equations developed for limestone in the literature were investigated. Estimated UCS values were calculated via appropriate conversions (Table 1). Similar to the SHR value evaluation

Table1 Estimated UCS value (MPa) according to the SHR value

Stone Samples	Average SHR Value	Conversion of SHR values into UCS values (MPa)						
		Via Conversion Table on Device	Calculation by Katz et al. 2000 [87]	Calculation by Kahraman 2001 [90]	Calculation by Fener et al. 2005 [88]	Calculation by Kılıç and Teymen 2008 [91]	Calculation by Yagiz, 2009 [89]	Updated average
Limestone-1	28	17.7	15.7	20.1	22.1	26.6	15.4	17.7
Limestone-2	42	37.3	41.8	34.1	50.5	66.8	43.8	45.4

[a] *SHR values obtained from the results of Schmidt hammer were transformed into UCS values with the help of formulas*

Table 2 Hardness classification of the stones

Stone samples	Average SHR value	Estimated UCS value (MPa)	Hardness class of stones by the SHR Value [71]
Limestone-1	28	17.7	Medium-hard (24–30)
Limestone-2	42	45.4	Hard (30–45)

criterion of the ASTM, values 7 units below and above the average were excluded from the evaluation. Accordingly, the values obtained from the equations developed by Katz et al. 2000, Fener et al. 2005, and Yagiz, 2009 were evaluated, and an average was again calculated [87–89] (Table 1).

To determine the rock strength and hardness classes of the limestones examined, a literature review was

Table 3 Rock strength classes according to the average SHR and estimated UCS values

Stone Samples		Average SHR Value	Rock strength class by ISRM 1981[a] [74]	Rock strength class by Waltham 2009[a] [92]	Rock strength class by Selby 1980[b] [72]
Limestone-1	17.7	28	Weak (5–25)	Medium (12.5–50)	Weak (10–35)
Limestone-2	45.4	42	Medium (25–50)	Medium (12.5–50)	Medium (40–50)

[a] In relevant literature, classification was made according to the UCS value

[b] Since a classification according to the SHR value exists in relevant literature, this value is used without conversion into the UCS

Table 4 Comparison of the estimated UCS values to reported limestone UCS values in the literature

UCS values of the limestone samples in the literature (MPa)		Limestone-1 estimated UCS value: 17.7 MPa	Limestone-2 estimated UCS value: 45.4 MPa
According to Hu et al. [93]	40.75–89.55	Below the limit	✓
According to Teymen [94]	40.9–140.9	Below the limit	✓
According to Şahin Güçhan et al. [95]	43.55–81.06	Below the limit	✓
According to Ünal and Beyaz [96]	7.40–16.20	✓	Above the limit
According to Şahin [97]	14.76–75.07	✓	✓
According to Gegenhuber et al. [98]	22.34–126.74	✓	✓
According to Akram and Bakar [99]	40.23–101.08	Below the limit	✓
According to Haftani et al. [100]	31.50–279.76	Below the limit	✓
According to Koç et al. [101]	Avg.: 13,97	✓	✓
According to Karaman and Kesimal [102]	7.7–18.9	✓	Above the limit
According to Dipova [103]	12.14–116.20	✓	✓
According to Tüysüz [104]	15.4–66.1	✓	✓
According to Marinos and Tsiambaos [105]	5.71–49.0	✓	✓
According to Ocak [106]	Avg.: 41.01	Below the average	✓
According to Waltham [92]	15–150	✓	✓

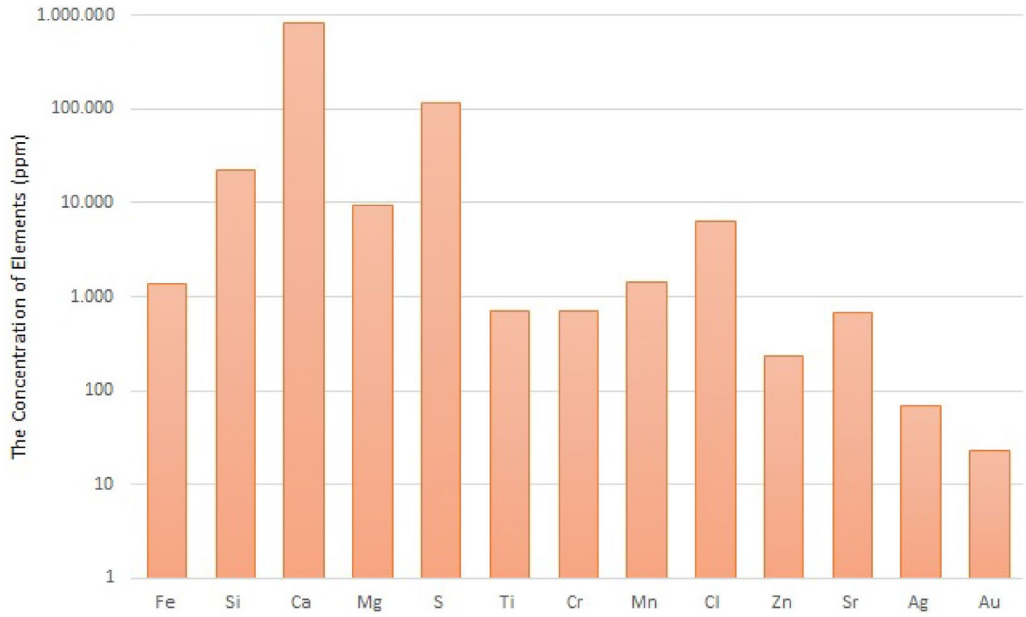

Fig. 18 Logarithmic graph of the element concentration in limestone-1

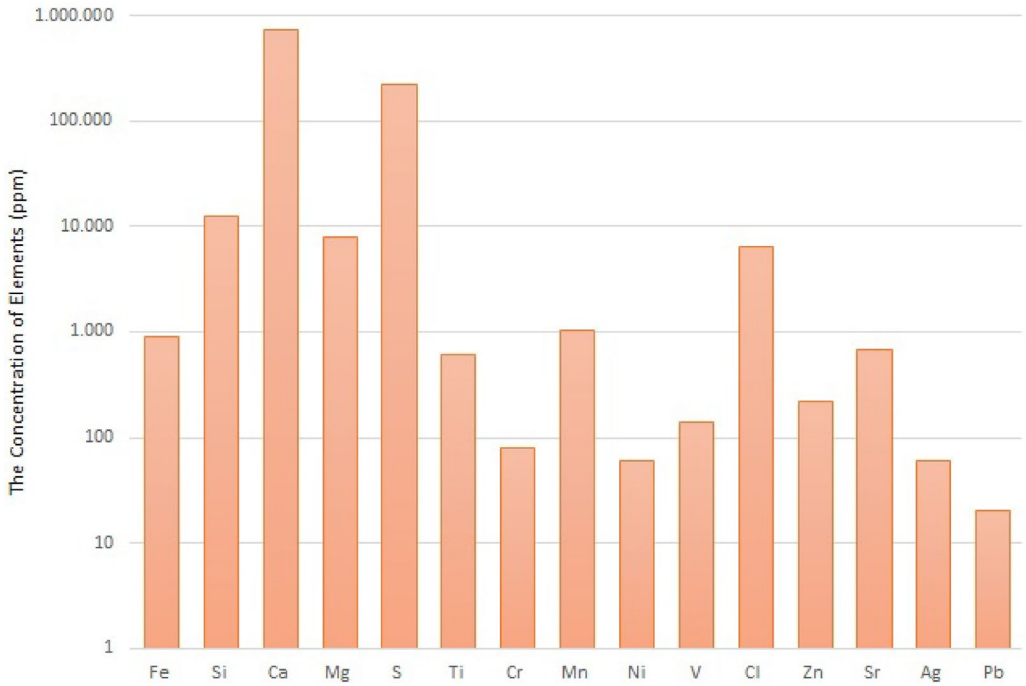

Fig. 19 Logarithmic graph of the element concentration in limestone-2

performed. Based on the estimated UCS values and average SHR values, the rock strength classes of the limestones could be determined, as listed in Table 2 and 3.

The SHR and UCS values of the limestones in zones 1 and 2 differed. Based on the hardness class, limestone-1 was defined as medium-hard rock, whereas limestone-2 was defined as hard rock; considering the strength class, according to ISRM [74] and Selby [72], limestone-1 was defined as weak rock, whereas limestone-2 was defined

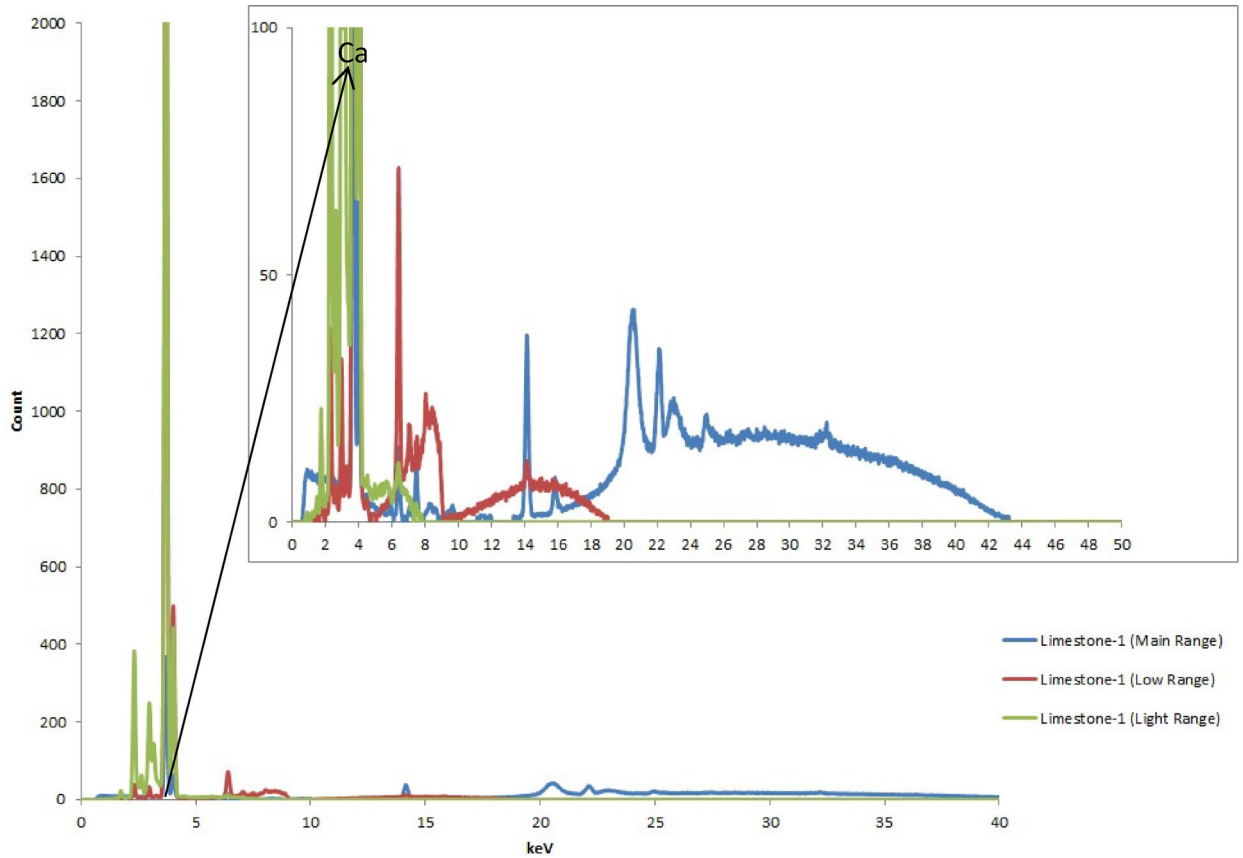

Fig. 20 XRF spectrum of limestone-1

as medium-hard rock, and according to Waltham 2009, both limestones were defined as medium-hard rocks.

A literature review was conducted of the UCS value of limestone, and the estimated UCS values of the two limestones in this study were compared to values reported in the literature. Accordingly, the estimated UCS value of limestone-2 agreed with the range of values in the literature and even exceeded two of these values. It could be concluded that this value was appropriate for limestone-2. The estimated UCS value of limestone-1 mostly remained within the range of values reported in the literature, and the estimate was lower than only a few of these values (Tables 3, 4).

X-Ray fluorescence (XRF) spectroscopy

Oxidized forms were extracted from the collected XRF data, and only the concentration of elements was calculated. When preparing graphs, elements that could not be detected during XRF analysis were not included, and the results were normalized according to ppm (Figs. 18, 19).

When the XRF spectrum graphs and logarithmic graphs of the element concentrations in limestone-1 and limestone-2 were evaluated (Figs. 18, 19, 20, 21), it was found that the concentration of Ca was very high in both stones (83.4–86.3%). Due to the difference in humidity, a variation in the Ca level of 2.9% was considered normal. The XRF device is a device that can only measure elements on the surface of the stone. Ca(OH)2 into CaCO3 transformation, which occurs in rock over time, affects the accumulation of Ca on the surface or within the stone. Because the elemental concentrations of limestone-1 and limestone-2 are the same, it was concluded that these both stones are the same type (Figs. 18, 19).

Mg, Fe and Mn occurred in trace amounts (less than 1%). Since the Mg ratio also indicated trace amounts, it could be concluded that these limestones are not dolomite. Mg is usually combined with carbonate, but here, Mg and Si were probably combined with OH. The analysed stones were clay–limestone, and the clay ratio was less than 1%. The amount of clay in the stone caused its colour to be yellowish white instead of pure white.

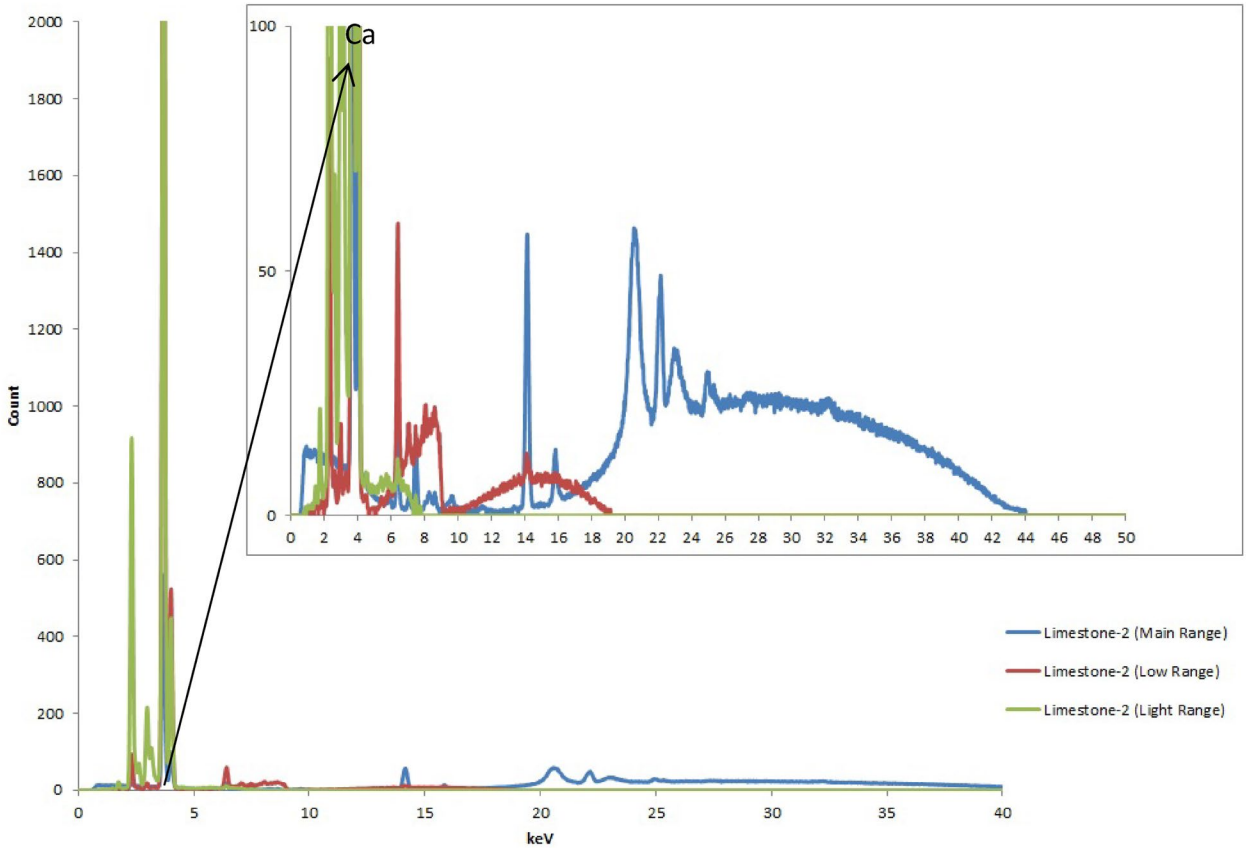

Fig. 21 XRF spectrum of limestone-2

The fact that limestone-1 included pitch-faced stones and limestone-2 included ashlar caused these stones to appear different in terms of shape, colour, and texture. In addition, their UCS and SHR values, strength and hardness classes, and average surface temperatures varied. However, when the graphs of the elemental concentration and XRF spectrum were evaluated, it could be concluded that these two stones are the same. In fact, it could be determined that these two stones were sourced from the same quarry, and only the stone-cutting process differed.

It is accepted that ashlar shaping is more laborious and costly than the shaping of pitch-faced stones. For this reason, in case of lack of financial resources, pitch-faced stone is used in the unimportant or invisible parts of the same building. Because the foundation level of this building was under the ground (not visible) in the years when it was built, it was built of pitch-faced stone [107, 108].

Stone hardens after extraction from the quarry. However, the occurrence of limestone-1 underground caused it to behave as if it still occurred at the quarry, but as a result of the exposure of limestone-2 above the ground level to atmospheric conditions, the stone absorbed CO_2, and carbonation occurred. The formation of $CaCO_3$ could explain the increased strength properties and hardness of limestone-2 [109–111]. The strength and hardness classes of both stones mostly remained within the limits reported in the literature. If evaluated from this perspective, it could be concluded that there is no serious problem in terms of the mechanical strength of the stones.

Ashlar also exhibited a lower visible cavities than when it was extracted from the quarry for the abovementioned reasons [109–111]. This caused rapid heat transmission, causing the temperature of ashlar to be lower than that of the pitch-faced stones.

Conclusion

The cultural heritage building researched in this study was examined without destruction, and this study aimed to encourage the application of NDT methods to other cultural heritage buildings.

IRT was applied on all the facades and invisible anomalies such as cavities underneath the plaster layer, joints, and material differences could be detected. Besides these,

deteriorations like blistering, formation of pores or plant, splitting make a significant thermal difference. Similar to the example in this article, as a result of IRT, stones may be perceived as different types of stones. However, when XRF analysis was performed, it was revealed that these stones were actually of the same type.

The innovation of this study is that although the infrared thermography technique is generally used in the investigation of materials, it was revealed that another technique such as XRF analysis is needed to better determine whether stones that appeared different based on IRT were actually different. While XRF analysis tells what the material is by presenting the elemental structure of the materials, IRT enables to detect invisible anomalies and physical deterioration of the materials. Therefore, the two techniques are not used interchangeably. They do not create an alternative to each other. In addition to these two techniques, SHR tests, which are non-destructive method, are also needed to give an idea about the mechanical features of the material. Therefore, when determining the conditions and for characterization analysis of a cultural heritage before restoration, different techniques should be jointly used to support each other.

The considered stones, which are located on the north side of the eastern façade of this building, are pitch-faced stones in the first 3 rows and ashlar stones in the next 2 rows. The fact that all 5 rows on the southern side of the same façade were entirely constructed of ashlar indicates that there was a slope from north to south at the time of building construction. In other words, it could be deduced that the topography of the building has changed. In addition, the emergence of stones at the foundation level years later caused these stones to be exposed to atmospheric conditions, resulting in their properties differing from those of the other stones. Cultural assets should be preserved not only considering the buildings themselves but also considering the environment in which they are located, even the topography. In this building example, it is recommended to return the building topography to the original conditions.

Abbreviations

NDT	Non-destructive testing
IRT	Infrared thermography
SHR	Schmidt hammer rebound
XRF	X-Ray fluorescence
UCS	Uniaxial compressive strength

Acknowledgements
I would like to thank Metallurgical and Materials Engineer Assoc. Prof. Dr. Ali ÖZER and Ali ALKAN, Director of Sivas Archeology Museum for their unwavering support in the conduct of these studies.

Author contributions
The author have role in the design of the study; in the collection, analyses, or interpretation of data; in the writing of the manuscript, or in the decision to publish the results. All authors read and approved the final manuscript.

Funding
This research did not receive any specific grant from funding agencies in the public, commercial, or not-for-profit sectors.

Availability of data and materials
The datasets used and/or analysed during the current study are available from the corresponding author on reasonable request.

Declarations

Competing interests
The author declares that she has no competing interests.

Received: 29 November 2022 Accepted: 21 February 2023
Published online: 28 March 2023

References

1. Ahunbay, Z. Tarihi Çevrede Koruma ve Restorasyon. İstanbul: Yapı Endüstri Merkezi Yayını. 2009.
2. Shrestha R, Sfarra S, Ridolfi S, Gargiulo G, Kim W. A numerical–thermal–thermographic NDT evaluation of an ancient marquetry integrated with X-ray and XRF surveys. J Therm Anal Calorim. 2022;147:2265–79.
3. Kilic G. Condition assessment of different historic bridges using non destructive techniques (NDT) with FTIR analysis in Izmir after the Samos Island earthquake. Herit Sci. 2022;10:111. https://doi.org/10.1186/s40494-022-00746-x.
4. Fort R, Feijoo J, Varas-Muriel MJ, Navacerrada MA, Barbero-Barrera MM, De la Prida D. Appraisal of non-destructive in situ techniques to determine moisture—and salt crystallization-induced damage in dolostones. J Build Eng. 2022;53: 104525.
5. Erkal A. Transmission of traffic-induced vibrations on and around the minaret of little Hagia Sophia. Int J Architect Herit. 2017;11(3):349–62.
6. Meng T, Huang R, Lu Y, et al. Highly sensitive terahertz non-destructive testing technology for stone relics deterioration prediction using SVM-based machine learning models. Herit Sci. 2021;9:24. https://doi.org/10.1186/s40494-021-00502-7.
7. Saint AC, Dritsa V, Koui M. Development of an optimized NDT methodology for the investigation of ancient greek copper-based artifacts. Corros Mater Degrad. 2021;2:325–40. https://doi.org/10.3390/cmd2020017.
8. Zendri E, Falchi L, Izzo FC, Morabito ZM, Driussi G. A review of common NDTs in the monitoring and preservation of historical architectural surfaces. Int J Architect Herit. 2017;11(7):987–1004. https://doi.org/10.1080/15583058.2017.1331477.
9. Zhang H, Sfarra S, Saluja K, et al. Non-destructive investigation of paintings on canvas by continuous wave terahertz imaging and flash thermography. J Nondestruct Eval. 2017;36:34. https://doi.org/10.1007/s10921-017-0414-8.
10. Sfarra S, Ibarra-Castanedo C, Ridolfi S. Holographic interferometry (HI), infrared vision and x-ray fluorescence (xrf) spectroscopy for the assessment of painted wooden statues: a new integrated approach. Appl Phys A. 2014;115:1041–56. https://doi.org/10.1007/s00339-013-7939-1.
11. Lechner T, Bjurhager I, Kliger RI. Strategy for developing a future support system for the vasawarship and evaluating its mechanical properties. Herit Sci. 2013;1:35. https://doi.org/10.1186/2050-7445-1-35.
12. Pürlü, K., Altın, Y., Aygün, A., Cebecioğlu, M., Özkanat, E., Çetindağ, E., Bedir, A., Kaya, A., Çavuş, İ., Babacan, S., Sivas 1000 Temel Eser, Sivas Kültür Envanteri The Cultural Inventory of Sivas]. Volume:1 (Merkez İlçe:

In (eds) Pürlü K., Sivas: Sivas Valiliği Sivas İl Kültür ve Turizm Müdürlüğü. 2011.
13. Akbulut G. Sivas Şehri'nin Tarihi Coğrafyası CÜ. Sosyal Bilimler Dergisi. 2009;35(2):212–22.
14. Demirel, Ö, Sivas, TDV İslâm Ansiklopedisi, 2009. 278–282.
15. Darkot, B, Sivas, İslam Ansiklopedisi. 1955. 569–577.
16. Kurtman F. Geologie Des Gebietes Zwischen Sivas und Divriği Sowie Bemerkungen Über Die Gipsserie. MTA Dergisi. 1961;56:1–12.
17. Koç H, Ergün A, Kartal F. Sivas ilinde bal üreticilerinin sorunları ve çözüm önerileri. Uluslararası Sosyal Bilimler Eğitimi Dergisi. 2020;6(2):327–62. https://doi.org/10.47615/issej.835332.
18. Google Earth Pro, kh.google.com. Accessed: 15 Mar 2022.
19. Meteorological Service, Republic of Turkey Minister of environment, urbanisation and climate change, meteorological Service. https://www.mgm.gov.tr/veridegerlendirme/il-ve-ilceler-istatistik.aspx?m=SIVAS. Accessed: 19 Mar 2022.
20. Kurtman F. Stratigraphie Der Gipsablagerungen Im Bereiche Von Sivas (Zentral - Anatolien). MTA Dergisi. 1961;56:13–6.
21. Dağlıyar A., Sivas İli Maden ve Enerji Kaynakları, Mineral research and exploration general directorate, (unpublished) 2010. https://www.mta.gov.tr/v3.0/sayfalar/bilgi-merkezi/maden_potansiyel_2010/sivas_madenler.pdf. Accessed: 20 Feb 2022
22. MTA, Sivas İli Maden Envanteri, Sivas: MTA Orta Anadolu I. Bölge Müdürlüğü. 2022. 416 (unpublished).
23. Bulut, M, Sivas'taki Geç Dönem Osmanlı Kamu Yapıları late period ottoman public buildings in Sivas. Sivas: Sivas Valiliği, İl Kültür ve Turizm Müdürlüğü Yayını. 2019. ISBN 978-975-17-4335-0.
24. Denizli, H, Sivas Tarihi ve Anıtları the history and monuments of Sivas. 170–171). Sivas: Özbelsan A.Ş. 1998. ISBN: 978–9759650902.
25. Başel, F, Sivas Bülteni, Sivas: Kamil Kitab ve Basım evi, 1935. 96.
26. Denizli H., Teknik ve Endüstri Meslek Lisesi Ağaç İşleri Atölyesi Raporu1983.
27. Pehlivan G, Conservin /Not Conserving cultural heritage by using, 4th International Conference of contemporary Affairs in architecture and Urbanism (ICCAUA-2021) 20–21 May 2021, 381–387.
28. Diz-Mellado E, Mascort-Albea EJ, Romero-Hernández R, Galán-Marín C, Rivera-Gómez C, Ruiz-Jaramillo J, Jaramillo-Morilla A. Non-destructive testing and finite element method integrated procedure for heritage diagnosis: the seville cathedral case study. J Build Eng. 2021;37: 102134.
29. Herschel W. Experiments on the solar, and on the terrestrial rays that occasion heat; with a comparative view of the laws to which light and heat, or rather the rays which occasion them, are subject, in order to determine whether they are the same, or different. Phil Trans R Soc. 1800. https://doi.org/10.1098/rstl.1800.0016.
30. Ring EFJ. The discovery of infrared radiation in 1800. Imaging Sci J. 2000;48(1):1–8. https://doi.org/10.1080/13682199.2000.11784339.
31. Pleşu R, Teodoriu G, Ţăranu G. Infrared thermography applications for building ınvestigation. Buletinul Institutului Politehn Din Iaşi. 2012;1:157–68.
32. Barbosa MTG, Rosse VJ, Laurindo NG. Thermography evaluation strategy proposal due moisture damage on building facades. J Build Eng. 2021;43:102555.
33. Ryms M, Tesch K, Lewandowski WM. The use of thermal imaging camera to estimate velocity profiles based on temperature distribution in a free convection boundary layer. Int J Heat Mass Transf. 2021;165: 120686.
34. An W, Yin X, Cai M, Tang Y, Li Q, Hu X. Influence of U-shaped structure on upward flame spread and heat transfer behaviors of PMMA used in building thermal engineering. Case Stud Ther Eng. 2020;22: 100794.
35. Sadhukhan D, Peri S, Sugunaraj N, Biswas A, Selvaraj DF, Koiner K, Rosener A, Dunlevy M, Goveas N, Flynn D, Ranganathan P. Estimating surface temperature from thermal imagery of buildings for accurate thermal transmittance (U-value): a machine learning perspective. J Buil Eng. 2020;32: 101637.
36. Vorajee N, Mishra AK, Mishra AK. Analyzing capacity of a consumer-grade infrared camera in South Africa for costeffective aerial inspection of building envelopes. Frontiers Architect Res. 2020;9:697–710.
37. Kishalı E, Türkmenoğlu Bayraktar N, Şener M. Kocaeli Tarihi Cami Örnekleri Üzerinden Planlı Koruma Kapsamında Hasarsız Test Uygulamaları: Çoban Mustafa Paşa Camii, Fevziye Camii ve Pertev Paşa Camii. METU JFA. 2019;36(1):107–36.
38. Lu X, Memari A. Application of infrared thermography for in-situ determination of building envelope thermal properties. J Build Eng. 2019;26:100885. https://doi.org/10.1016/j.jobe.2019.100885.
39. Lewandowski WM, Ryms M, Denda H. Quantitative study of free convective heat losses from thermodynamic partitions using thermal ımaging. Energy Build. 2018;2018167:370–83.
40. Golasi KM, Pieczyska E, Staszczak M, Maj M, Furuta T, Kuramoto S. Infrared thermography applied for experimental investigation of thermomechanical couplings in gum metal. Quant InfraRed Therm J. 2017;14(2):226–33.
41. Szajewska A. Development of the thermal imaging camera (TIC) technology. Procedia Eng. 2017;172:1067–72.
42. Troppová E, Klepárník J, Tippner J. Thermal bridges in a prefabricated wooden house: comparison between evaluation methods. Wood Mater Sci Eng. 2016;11(5):305–11.
43. Huh J, Tran QH, Lee JH, Han DY, Ahn JH, Yim S. Experimental study on detection of deterioration in concrete using ınfrared thermography technique. Adv Mater Sci Eng. 2016. https://doi.org/10.1155/2016/1053856.
44. Albatici R, Tonelli AM, Chiogna M. A comprehensive experimental approach for the validation of quantitative infrared thermography in the evaluation of building thermal transmittance. Appl Energy. 2015;141:218–28. https://doi.org/10.1016/j.apenergy.2014.12.035.
45. Mercuri F, Cicero C, Orazi N. Infrared thermography applied to the study of cultural heritage. Int J Thermophys. 2015;36:1189–94. https://doi.org/10.1007/s10765-014-1645-x.
46. Ohlsson KEA, Olofsson T. quantitative infrared thermography imaging of the density of heat flow rate through a building element surface. Appl Energy. 2014;134:499–505.
47. Kylili A, Fokaides PA, Christou P, Kalogirou SA. Infrared thermography (IRT) applications for building diagnostics: a review. Appl Energy. 2014;134:531–49.
48. Bektaş Ekici, B, Binalarda Güneş Isısı Kazanç Faktörü ve Yüzey Sıcaklıklarının Saydam ve Opak Yüzey Tasarımına Etkisinin Deneysel Olarak Araştırılması. Yayımlanmamış yüksek lisans tezi). Fırat Üniversitesi Fen Bilimleri Enstitüsü, Elazığ. 2012.
49. Fokaides PA, Kalogirou SA. Application of Infrared thermography for the determination of the overall heat transfer coefficient (U-Value) in building envelopes. Appl Energy. 2011;88:4358–65.
50. Zalewski L, Lassue S, Rousse D, Boukhalfa K. Experimental and numerical characterization of thermal bridges in prefabricated building walls. Energy Convers Manag. 2010;51(12):2869–77.
51. Amon F, Hamins A, Bryner N, Rowe J. Meaningful performance evaluation conditionsfor fire service thermal imaging cameras. Fire Saf J. 2008;43(8):541–50.
52. Chown GA, Burn KN. Thermographic ıdentification of building enclosure effects and deficiencies Canadian building digest. Resolve. 1983. https://doi.org/10.4224/40000723.
53. Griffin I, Tate J. Conserving our wartime heritage. J Archit Conserv. 2012;18(1):81–100. https://doi.org/10.1080/13556207.2012.10785105.
54. Tavakolian P, Shokouhi BE, Sfarra S, Gargiulo G, Mandelis A. Non-destructive imaging of ancient marquetries using active thermography and photothermal coherence tomography. J Cult Heritage. 2020;46:159–64.
55. Pettersson B, Axen B, Thermography-testing of the thermal insulation and airtightness of buildings Swedish Council for building research. Stockholm: Spfmgbergs Tryckerier AB. 1980.
56. Balaras CA, Argiriou AA. Infrared thermography for building diagnostics. Energy Build. 2002;34(2):171–83.
57. Sarıtabak, E., Bina Kabuğunun Dış Duvarları ve Ara Kesitlerinde Isıl Ve Nemsel Performansın Kızılötesi Termografi İle Değerlendirilmesi Üzerine Bir Alan Çalışması. Yayımlanmamış yüksek lisans tezi İTÜ Fen Bilimleri Enstitüsü, İstanbul. 2012.
58. Li Z, Yao W, Lee S. Application of infrared thermography technique in building finish evaluation. J Nondestr Eval. 2000;19:11–9.
59. Bayraktar TN, Kishalı E. Tarihi Yapılarda Hasarsız Testler Aracılığıyla Önleyici Korumanın Sağlanması: Kocaeli Ulugazi İlkokulu Örneği. Mimarist. 2017;60:85–90.
60. Meteorological Service, Republic of Turkey Minister of Environment, Urbanisation and Climate Change, Meteorological Service. https://

www.mgm.gov.tr/veridegerlendirme/il-ve-ilceler-istatistik.aspx?m=SIVAS. Accessed 12 June 2021.
61. The Weather Channel, weather.com. Accessed 18 Jan 2022
62. ICOMOS. 2008 Illustrated glossary on stone deterioration patterns, ICOMOS International scientific committee for stone (ISCS) Ateliers 30 Impression Champigny/Marne. https://doi.org/10.1016/j.conbuildmat.2018.10.180
63. Kong F, Xue Y, Qiu D, Gong H, Ning Z. Effect of grain size or anisotropy on the correlation between uniaxial compressive strength and Schmidt hammer test for building stones. Constr Build Mater. 2021;299: 123941.
64. Karaman K, Erçıkdı B, Cihangir F, Kesimal A. Examining the schmidt hammer methods in estimation of the uniaxial compressive strength Türkiye 22. Uluslararası Madencilik Kongresi ve Sergisi 11–13 May 2011 Ankara. 2011. https://www.researchgate.net/publication/267781874
65. Mohammed AD, Alshkane YM, Hamaamin YA. Reliability of empirical equations to predict uniaxial compressive strength of rocks using Schmidt hammer. Georisk Assess Manage Risk Eng Syst Geohazards. 2020. https://doi.org/10.1080/17499518.2019.1658881.
66. Vasanelli E, Colangiuli D, Calia A, Sbartaï Z, Breysse D. Combining noninvasive techniques for reliable prediction of soft stone strength in historic masonries. Constr Build Mater. 2017;146:744–54.
67. Sy´kora M, Diamantidis D, Holicky´ M, Marková J, Rózsás Á. Assessment of compressive strength of historic masonry using non-destructive and destructive techniques construction and building materials. 2018
68. Parsajoo M, Armaghani DJ, Mohammed SA, Khari M, Jahandari S. Tensile strength prediction of rock material using non-destructive tests: a comparative intelligent study transportation geotechnics. Construct Build Mater. 2021;31:100652.
69. Poblet J, Bulnes M, Uzkeda H, Mag´an M. Using the schmidt hammer on folds: an example from the cantabrian zone (NW Iberian Peninsula). J Struct Geol. 2022;155:104512.
70. Schmidt E. A non-destructive concrete tester. Concrete. 1951;59(8):34–5.
71. De Beer, J. H., Subjective classification of the hardness of rocks and the associated shear strength, Proceedings of 4th reg cong Afr soil mechanical found engineering. Capctawn. 1967. 396–398.
72. Selby MJ. A rock mass strength classification for geomorphic purposes: with test from Antarctica and New Zealand. Z Geomorphol. 1980;24:31–51.
73. Waltham T. Foundations of engineering geology. London: Spon Press Taylor & Francis; 2009.
74. ISRM. Rock characterization, testing and monitoring. Los Angeles: International Society for Rock Mechanics Suggested Methods; 1981.
75. Saptono S, Kramadibrata S, Sulistianto B. Using the schmidt hammer on rock mass characteristic in sedimentary rock at tutupan coal mine. Proced Earth Planet Sci. 2013;6:390–5.
76. Atkinson RH, Hudson JA. Hardness tests for rock characterization a chapter in comprehensive rock engineering. Oxford: Pergamon Press; 1993.
77. Donais MK, Alrais M, Konomi K, George D, Ramundt WH, Smith E. Energy dispersive X-ray fluorescence spectrometry characterization of wall mortars with principal component analysis: Phasing and ex situ versus in situ sampling. J Cult Herit. 2020;43:90–7. https://doi.org/10.1016/j.culher.2019.12.007.
78. Chirco G, Portale EC, Caponetti E, Renda V, Chillura MD. Investigation on four centuripe vases by portable X-ray fluorescence and total reflectance-FTIR. J Cult Heritage. 2021;8:326–35. https://doi.org/10.1016/j.culher.2020.10.011.
79. Pehlivan E. Archaeological evaluation and provenance analysis of apollon's torso in sivas archaeological museum. Mediter Archaeol Archaeom. 2022;22(1):xx–xx.
80. Mitsos D, Kantarelou V, Palamara E, Karydas AG, Zacharias N, Gerasopoulos E. Characterization of black crust on archaeological marble from the library of Hadrian in Athens and inferences about contributing pollution sources. J Cult Heritage. 2022. https://doi.org/10.1016/j.culher.2021.12.003.
81. Radepont M, Échard JP, Ockermüller M, Codre H, Belhadj O. Revealing lost 16th century royal emblems on two Andrea Amati's violins using XRF scanning. Herit Sci. 2020;8:112. https://doi.org/10.1186/s40494-020-00460-6.
82. Sumner P, Nel W. The effect of moisture on schmidt hammer rebound: tests on rock samples from marion Island and South Africa. Earth Surf Proc Landforms. 2002;27:1137–42.
83. ASTM, Standard test method for determination of rock hardness by rebound hammer method**.** ASTM Stand. 2019. D 5873–05.
84. ISRM. The Complete ISRM suggested methods for rock characterization. In: Ulusay RJA, Hudson, editors. Testing and Monitoring. Ankara: Kozan Offset Press; 2007.
85. Matthews JA, Winkler S, Wilson P. Age and origin of ice-cored moraines in jotunheimen and breheimen, southern norway: insights from schmidt-hammer exposure-age dating. Geogr Ann Ser B. 2014;96:531–48. https://doi.org/10.1111/geoa.12046.
86. USBR. Engineering geology field manual. Field İndex Tests. 1998;1:111–20.
87. Katz O, Rechesa Z, Roegiersc JC. Evaluation of mechanical rock properties using a Schmidt hammer. Int J Rock Mech Min Sci. 2000;37(4):723–8.
88. Fener M, Kahraman S, Bilgil A, Gunaydin O. A comparative evaluation of indirect methods to estimate the compressive strength of rocks. Rock Mech Rock Eng. 2005;38(4):329–43.
89. Yagiz S. Predicting uniaxial compressive strength, modulus of elasticity and index properties of rocks using the Schmidt hammer. Bull Eng Geol Environ. 2009;68(1):55–63.
90. Kahraman S. Evaluation of simple methods for assessing the uniaxial compressive strength of rock. Int J Rock Mech Min Sci. 2001;38(7):981–94.
91. Kılıç A, Teymen A. Determination of mechanical properties of rocks using simple methods. Bull Eng Geol Environ. 2008;67:237–44.
92. Waltham T. Foundations of engineering geology. London: Spon Press Taylor & Francis; 2002.
93. Hu Z, Wen T, Zheng K, Wang Y. A Method for determining the mechanical parameters of solution pore and crevice limestone based on porosity. Adv Civil Eng. 2021;2021:1687–8086. https://doi.org/10.1155/2021/8833370.
94. Teymen A. Estimation of uniaxial compressive strength of very low-medium abrasive rocks from Cerchar abrasiveness index. Pamukkale Univ Muh Bilim Dergi. 2020;26(6):1154–63.
95. Şahin Güçhan N, Bilecen K, Warscheid T, Topal T, Son Ç, Çıplak E. S, Ersöz T, Kaya Y, Öztürk M, Tarihi Kireçtaşlarını Koruma Müdahalelerinde Uygulamak Üzere Kalsit Üreten Bakterilerle Biyolojik Harç Geliştirilmesi, Program Kodu: 1001, Proje No: 115M188, Ankara: TÜBİTAK ARDEB. 2019.
96. Ünal M, Beyaz T. Hasankeyf Kireçtaşlarının Suda Dağılmaya ve Tuz Kristalleşmesine Karşı Direncinin Araştırılması. Eng Sci. 2019;14(2):55–62.
97. Şahin M, Nokta Yükü Dayanım İndeksinin Yarılanmış Karot Örneklerinden Belirlenebilirliğinin Araştırılması, Hacettepe Üniversitesi, Jeoloji Mühendisliği Anabilim Dalı, 2018
98. Gegenhuber N, Schifko T, Pittino G. Petrographic coded model concept for the correlation between geomechanical and elastic properties and its application on log data for Alpine rocks. Aust J Earth Sci. 2017;110(1):101–8. https://doi.org/10.17738/ajes.2017.0007.
99. Akram, M.S., & Bakar, MZ. Correlation between uniaxial compressive strength and point load ındex for salt-range rocks. Journal of Engineering and Applied Sciences. 2016.
100. Haftani M, Bohloli B, Nouri A, MalekiJavan RM, Moosavi M. Size effect in strength assessment by indentation testing on rock fragments. Int J Rock Mech Min Sci. 2014;65:141–8.
101. Koç E, Demir Şahin D. and Yılmaz A. O, Examination of Indirect tensile and point load strength on different originated rock samples taken between Trabzon-Maçka Areas, KAYAMEK'2014-XI. Bölgesel Kaya Mekaniği Sempozyumu/ROCKMEC'2014-XI th regional rock mechanics Symposium. Afyonkarahisar. Turkey. 2014.
102. Karaman K, Kesimal A. Kayaçların Tek Eksenli Basınç Dayanımı Tahmininde Nokta Yükü Deney Yöntemleri ve Porozitenin Değerlendirilmesi. Madencilik. 2012;51(4):3–14.
103. Dipova N. Investigation of the relationships between abrasiveness and strength properties of weak limestones along a tunnel route. Jeoloji Mühendisliği Dergisi. 2012
104. Tüysüz L, İstanbul'da Açılacak Metro Tünellerinde Tbm (Tünel Açma Makinesi) Performansını Tahmin Etmek İçin Yeni Bir Yaklaşım, İstanbul

Teknik Üniversitesi, Fen Bilimleri Enstitüsü, Maden Mühendisliği Anabilim Dalı, Yüksek Lisans Tezi, 2012.
105. Marinos V, Tsiambaos G. Strength and deformability of specific sedimentary and ophiolithic rocks. Bull Geol Soc Greece. 2010;43:1259–66.
106. Ocak İ. Tek Eksenli Basınç Dayanımını Kullanarak Kaya Malzemesinin Elastisite Modülünün Tahmini. İstanbul Yerbilimleri Dergisi. 2008;21(2):91–7.
107. Gündüz, S, Osmanlı Beyliği Mimarisinde Anadolu Selçuklu Geleneği. Yayımlanmamış doktora tezi. Hacettepe Üniversitesi Sosyal Bilimler Enstitüsü, Ankara. 2006.
108. Kutlu M, XIV-XV. Yüzyıllara Ait Osmanlı Camilerinde Görülen Tuğla-Taş Almaşıklığı Üzerine Gözlemler, Sanat Tarihi Dergisi. 2017
109. Arıoğlu N. and Arıoğlu E, Mimar Sinan'ın Seçtiği Taş: Küfeki ve Çekme Dayanımı", Türkiye İnşaat Mühendisliği 14. Teknik Kongresi, 1993. 1021–1034
110. Arıoğlu E. and Arıoğlu N, Mimar Sinan'ın Taşıyıcı Olarak Kullandığı Küfeki Taşının Mühendislik Gizemi", Mimar Sinan Dönemi Yapı Teknikleri Seminer, Yapı Merkezi, Mayıs 1999, İstanbul, 1999. 2–20.
111. Kumral M, Şans G, Yalçın C, Kaya M, Budakoğlu M. Çatalca (İstanbul) Civarındaki Tarihi Küfeki Taşının Oluşumunda Fiziksel ve Kimyasal Özelliklerin Etkileri Omer Halisdemir University. J Eng Sci. 2019;8(1):278–87.

Publisher's Note